Supplementary Information

Machine-learning-assisted discovery of polymers with high thermal conductivity using a molecular design algorithm

Stephen Wu, Yukiko Kondo, Masa-aki Kakimoto, Bin Yang, Hironao Yamada, Isao Kuwajima, Guillaume Lambard, Kenta Hongo, Yibin Xu, Junichiro Shiomi, Christoph Schick, Junko Morikawa, Ryo Yoshida

This document provides detailed information on transfer learning models, process of molecule design, and experimental validation, including the polymer synthesis details of the three finally selected candidates.

1 Performance of transfer learning

As described in the main text, we produced 1,000 pre-trained neural networks with respect to each of T_{g}, T_{m}, and ρ for polymers and C_{V} for monomers. All these models were transferred to those predicting λ using a randomly chosen 80% of the given 28 samples as training instances and the remaining 20% as testing instances. The random splitting of data was repeated five times to evaluate the generalization capabilities of the transferred models (i.e., Pearson's correlation and mean absolute error (MAE)), as shown in Fig. S1. Fig. S2 shows the prediction versus observation plot of the best-performing model for the transfer from each source property. Overall, the transfer from the monomeric C_{V} to λ reached the best MAE. Therefore, we used this model during the post-screening step of our design process.

2 Molecular design process

Supplementary Movie S1 shows the dynamic process of modifying the chemical structures with the desired range, $T_{\mathrm{g}} \in \{200, 500\}$ and $T_{\mathrm{m}} \in \{300, 600\}$, starting from 100 initial seeds taken from PoLyInfo. Red circles represent the experimental properties of existing polymers, which were used in the training process, and blue circles represent the predicted properties of the designed structures that were placed in the top 25 in terms of realized likelihood values at each step of the iteration.

3 Selected candidates

Table S1 summarizes the predicted properties of the 24 selected candidates whose chemical structures are shown in Fig. S3.

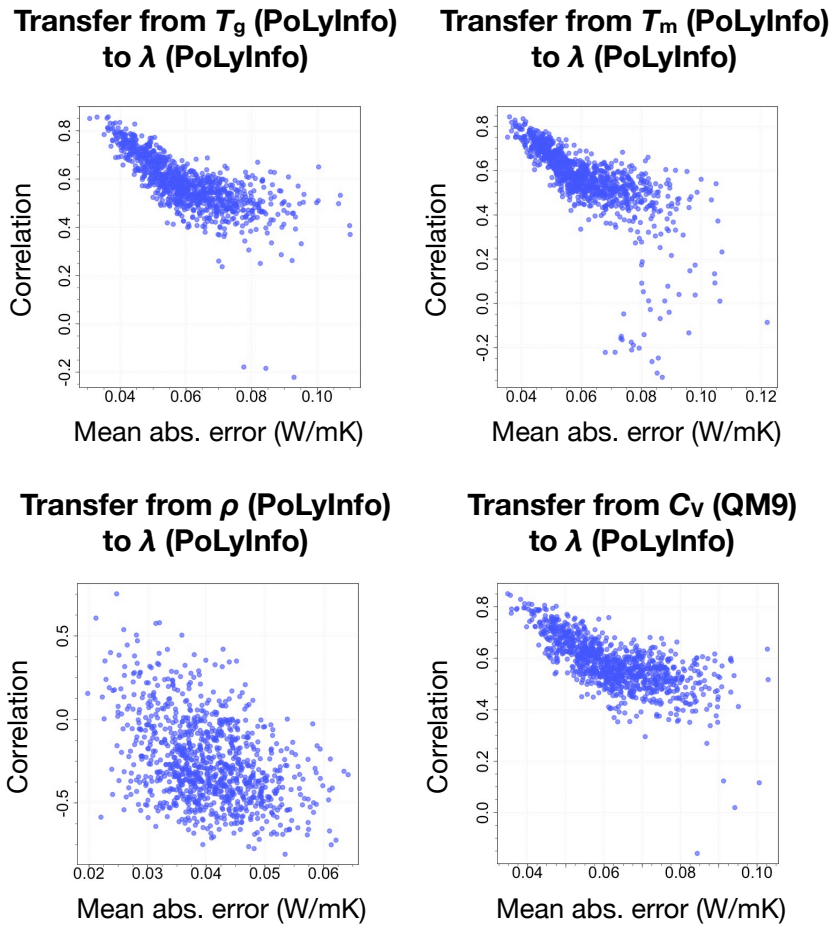

Figure S1: MAE and Pearson's correlation coefficients of the predicted λ with respect to the 28 observations that were calculated by the transferred models from T_g, T_m, ρ, and monomeric C_V, respectively.

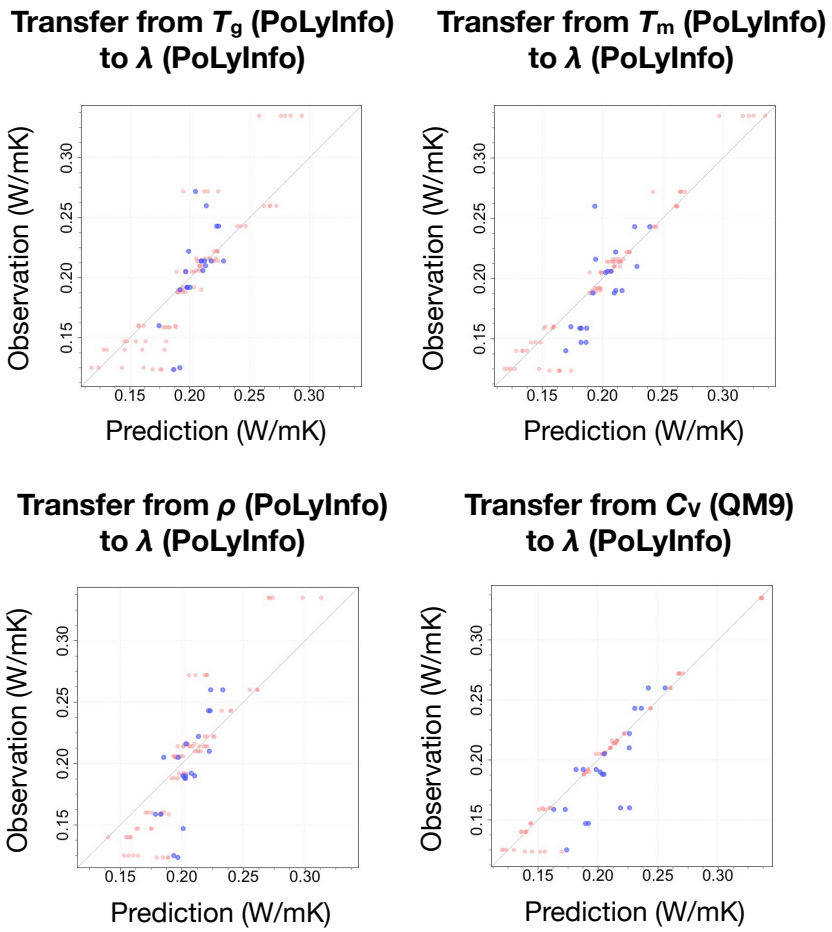

Figure S2: Prediction and observation plots for the transferred models on λ, whose source models were trained on different data sets with regard to T_{g}, T_{m}, ρ, and monomeric C_{V}, respectively.

Table S1: Predicted property values of the 24 selected candidates.

Polymer	SA	T_g (°C)	T_m (°C)	ρ (g/cm^3)	λ (W/mK)
1	3.41	248.6	465.6	1.331	0.237
2	2.55	141.7	408.1	1.220	0.234
3	2.61	272.3	440.9	1.290	0.228
4	3.70	286.4	403.7	1.308	0.246
5	3.78	279.0	309.4	1.260	0.233
6	1.46	184.3	333.8	1.278	0.214
7	2.52	255.8	275.2	1.264	0.227
8	2.56	171.8	328.1	1.212	0.195
9	2.91	365.1	487.9	1.325	0.223
10	2.43	176.5	398.2	1.209	0.226
11	2.76	277.9	513.6	1.259	0.225
12	2.41	181.3	417.5	1.218	0.197
13	2.17	228.3	426.1	1.288	0.225
14	2.23	199.6	439.8	1.224	0.222
15	2.58	160.8	374.3	1.196	0.206
16	2.82	187.6	520.3	1.256	0.228
17	2.88	201.6	459.6	1.282	0.225
18	2.33	245.8	399.3	1.273	0.218
19	1.70	121.5	321.0	1.260	0.218
20	4.33	137.5	346.3	1.274	0.213
21	2.37	166.6	353.4	1.266	0.213
22	2.21	136.6	230.7	1.188	0.222
23	3.15	185.3	421.7	1.281	0.231
24	2.81	123.9	351.0	1.251	0.236

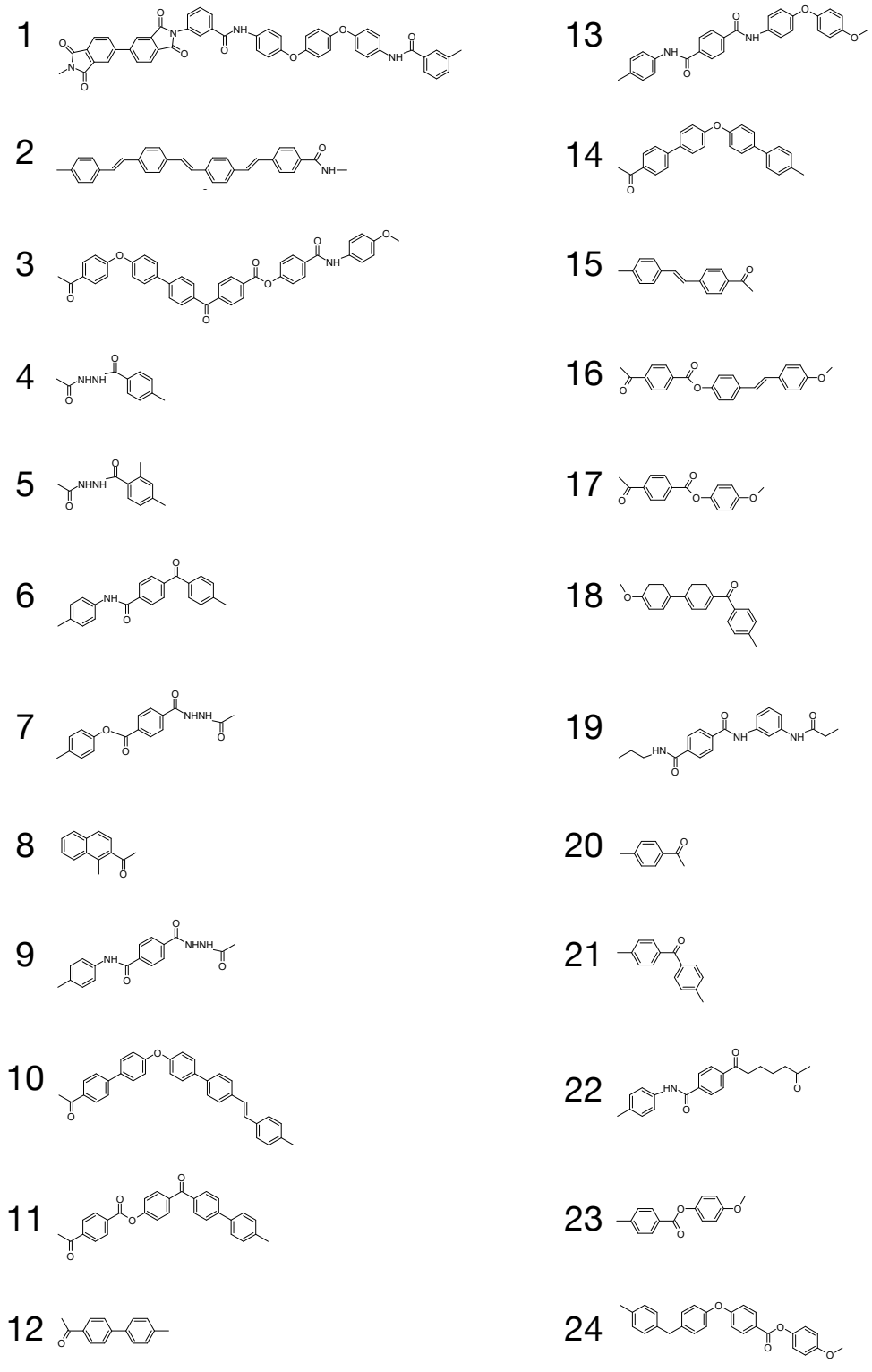

Figure S3: Chemical structures of the repeat units of the 24 computationally designed polymers.

4 Experimental validation

This section summarizes all details of experiments performed in this study. Table S2 summarizes all the material properties tested on the three newly synthesized polymers.

Table S2: Experimental properties of the three newly synthesized polymers compared with predictions from machine learning models (α: thermal diffusivity, C_P: specific heat capacity, ρ: density, λ: thermal conductivity, η_{inh}: inherent viscosity, TG_{10}: temperature of the weight loss 10%, Xc: crystallinity). Compressed film-shaped samples were used in all cases except the X-ray diffraction of polymer 19a. We report values from prediction (pre), observation (obs), and observation after annealing (anneal). (* DSC failed to measure T_g values, and instead, FSC was introduced to determine T_g and T_m. ** Thermal conductivity of annealed polymer 4 was obtained using the heat capacity and density measured for non-heat-treated samples. # Xc of polymer 19a was measured in powder form).

Polymer	4 (pre)	4 (obs)	4 (anneal)	13(pre)	13 (obs)	13 (anneal)	19 (pre)	19a (obs)
T_g (°C) (DSC)	286	N/A*	-	228	N/A*	-	121	194
T_g (°C) (FSC)	286	221	-	228	226	-	121	191
T_m (°C) (FSC)	404	513	-	426	494	-	321	303
α (mm^2/s)	-	0.168	0.263	-	0.152	0.254	-	0.133
C_P (at 25–27°C)	-	1.13	-	-	1.14	1.10	-	1.19
ρ (at 16–20°C)	1.308	1.373	-	1.288	1.295	1.386	1.260	1.233
λ (W/mK)	0.246	0.261	0.408**	0.225	0.224	0.387	0.218	0.195
η_{inh} (dL/g)	-	0.193	-	-	0.317	-	-	0.313
TG_{10} (°C)	-	400	-	-	>500	-	-	361
Xc	-	0.16	-	-	0.30	0.30	-	0.09#

4.1 Measurements

Infrared (IR) absorption spectra of polymers were measured by the KBr tablet method using Fourier transform IR spectroscopy (FTIR) on a Perkin Elmer Spectrum One (Massachusetts, USA). The attenuated total reflection (ATR) IR method was applied to measure the IR reflection spectra of compressed thick samples. Proton (^1H) nuclear magnetic resonance (NMR) spectra were recorded using a JEOL ECS-400 (Tokyo, Japan) with dimethyl sulfoxide-d_6 (DMSO-d_6) as a solvent. The inherent viscosity (η_{inh}) of polymers was measured at 0.5 g/dL in *N*,*N*-dimethylacetamide(DMAc) or in concentrated sulfonic acid solutions at 30°C with an Ostwald viscometer. Thermal gravimetric analysis (TGA) and differential scanning calorimetry (DSC) were performed using a Perkin Elmer TGA7 and a Perkin Elmer DSC7, respectively, at a heating rate of 10°C/min under a nitrogen atmosphere. The specific heat (C_P) of polymers was calculated by a simple comparison of the heat flow rates into a sample and a calibration substance (sapphire) by the classical three-step technique in a temperature range of 20–50°C using DSC. Thermo-mechanical analysis (TMA) was undertaken using a SEIKO (Tokyo, Japan) TMA - SS-6000 to measure thermal expansion at a heating rate of 5°C/min under ambient atmospheric conditions. The crystallinity of powder or compressed pellet samples was determined by a Rigaku (Tokyo, Japan) wide-angle X-ray diffraction (WAXD) Mini Flex 600. The thermal diffusivity of the synthesized polymers was measured by the temperature wave method using an ai-Phase mobile 1 supplied by ai-Phase Co. Ltd. (Tokyo, Japan). The density was determined by Archimedes' method using an electronic densimeter SD-200L supplied by Alpha Mirage Co. Ltd. (Tokyo, Japan).

T_g of polymer 19a was 194°C, as measured by differential scanning calorimetry (DSC). In contrast, the crystallinity of polymers 4 and 13 was 16% and 30%, respectively, as obtained by WAXD of compressed pellet samples. Although T_g of polymer 19a was observed clearly by DSC, no clear T_g value was measured in the cases of polymers 4 and 13 in compressed pellets using a thermal mechanical analyser (TMA). The predicted values of T_g of polymers 4, 13, and 19a were 286°C, 228°C, and 122°C, respectively. As discussed

below, by introducing fast scanning calorimetry (FSC), T_g and T_m of all three polymers were successfully observed.

The compressed pellet thermal conductivities of polymers 4 and 13 were 0.26 W/mK and 0.22 W/mK at room temperature (r.t.), respectively. However, after annealing at 400°C, these values increased by more than 50% to 0.41 W/mK and 0.39 W/mK, respectively.

4.2 Reagents

Terephthaloyl chloride M1, terephthalic dihydrazide M2,terephthalic acid M3, 1,4-bis(4-aminophenoxy)benzene M4, *m*-phenylene diamine M7,3-aminobutanoic acid M8, benzylalcohol M9, triphenylphosphite, pyridine, triethylamine, palladium on carbon (10 w%), and toluene sulfonic acid were sourced from Tokyo Chemical Industry. Anhydrous grade solvents, namely, dichloromethane (DMC), ethylacetate, *N*,*N*-dimethylacetamide (DMAc), and *N*-methylpyrrolidone (NMP), were also purchased from Tokyo Chemical Industry. Terephthaloyl chloride was purified by sublimation, and other reagents and solvents were used as received.

4.3 Preparation of monomers and polymers

Preparation of polymer 4

In a flask, 1.94 g (10 mmol) of terephthalic dihydrazide M2 was dissolved in 30 mL of NMP under N_2. Next, 2.03 g (10 mmol) of terephthaloyl chloride M1 dissolved in 10 mL of NMP was added under cooling by ice bath. The solution was stirred overnight at r.t. and then added to 500 mL of methanol. The obtained powdery polymer was dried at 100°C under reduced pressure. The yield of polymer 4 was 2.79 g (86%). This polymer was insoluble in organic solvents. The inherent viscosity was 0.192 dL/g measured at 30°C concentration of 5 g/L in conc. sulfuric acid. Elemental analysis: Cal. C, 59.3%, H, 3.7%, N, 17.3%, Obs. C, 55.6%, H, 3.9%, N, 16.9%. The IR spectrum is shown in Fig. S4a.

Preparation of polymer 13

In a flask, 0.83 g (5 mmol) of terephthalic acid M3 was dissolved in 8 mL of NMP containing 0.5 g of lithium chloride under a nitrogen atmosphere (N_2). Next, 1.46 g (5 mmol) of 1,4-bis(4-aminophenoxy)-benzene M4, 3.10 g (5 mmol) of triphenyl phosphite, 2.5 mL of pyridine, and finally 1 mL of NMP for washing the flask were added consecutively. The mixture was stirred for 3 h at 100°C under a nitrogen atmosphere. White precipitate was observed during the reaction. After the solution was cooled to r.t., it was added to 350 mL of methanol. The solid polymer was separated by filtration and washed in boiling methanol. The obtained powdery polymer was dried at 100°C under reduced pressure. The yield was 2.05 g (97%), and this polymer was insoluble in organic solvents. The inherent viscosity measured at 30°C concentration of 5 g/L in conc. sulfuric acid was 0.317 dL/g. Elemental analysis: Cal. C, 73.9%, H, 4.3%, N, 6.6% Obs. C, 71.9%, H, 4.1%, N, 6.4%. The IR spectrum is shown in Fig. S4b.

Preparation of monomer M6

Monomer M6, the monomer for polymer 19a, was developed as shown in Fig. S5. Terephthaloyl chloride mono-benzyl ester was prepared in situ from terephthaloyl chloride M1 and an equi-molar amount of benzyl alcohol M9. Then, the benzyl ester of p-toluene sulfonic acid salt M10, which was synthesized by ordinary amino acid esterification starting from 3-aminobutanoic acid M8, was reacted in the solution to obtain dibenzyl ester M11, the precursor of monomer M6.

A mixture of 2.70 g (25 mmol) of benzyl alcohol M9 and 3.17 g of triethylamine in 20 mL of DMC was added to a 5.075 g (25 mmol) solution of terephthaloyl chloride M1 in 100 mL of DMC at r.t. This mixture was then refluxed for 2 h under a nitrogen atmosphere. After the mixture was cooled to r.t., 9.14 g of benzylester M10 and 6.33 g of triethylamine in 50 mL of DMC was added, and the mixture was stirred at r.t. for 3 h. The resulting reaction mixture was washed with water. DMC was evaporated under reduced

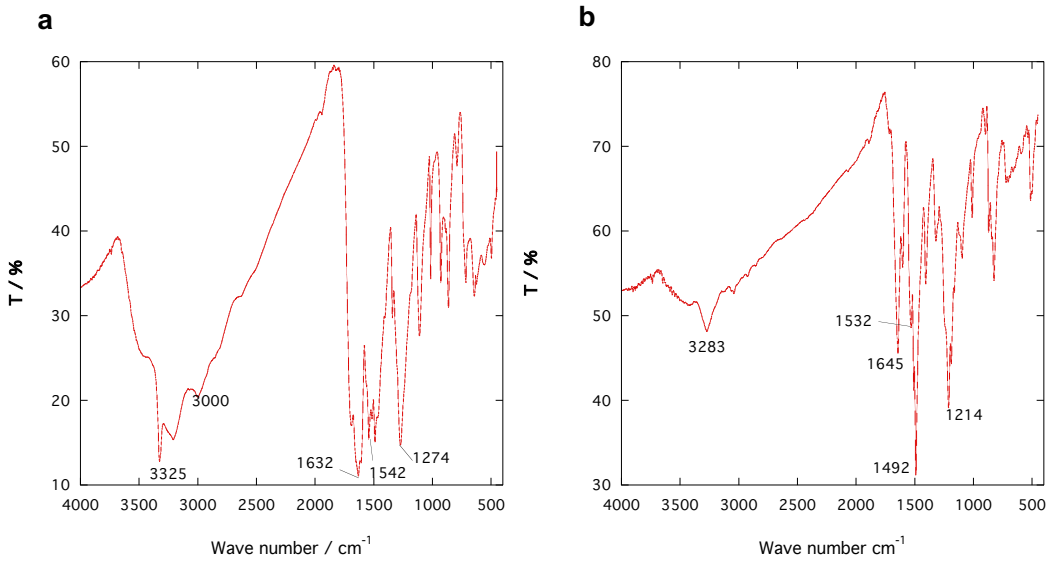

Figure S4: (a) FTIR spectrum for polymer 4. (b) FTIR spectrum for polymer 13.

pressure after the solution was dried by anhydrous $MgSO_4$. Compound M11 was obtained by silica gel column chromatography using ethyl acetate as an eluent. The yield was 4.70 g (44%).

Next, 4.32 g (10 mmol) of M11 and 1.06 g (1 mmol) of palladium on carbon (10 w%) was mixed with 50 mL of ethyl acetate. The flask atmosphere was replaced by hydrogen, and the solution was stirred for 2 days. After the gas in the flask was replaced by nitrogen, 100 mL of 1 M aqueous solution of sodium hydroxide was added to the reaction mixture. The black-coloured catalyst was removed by filtration, and the filtrate was acidified using 1 M hydrochloric acid. Monomer M6 was obtained as precipitate. The yield was 753 mg (30%). The IR spectrum is shown in Fig. S6a and the NMR spectrum in Fig. S6b.

Preparation of polymer 19a

Polyamide 19a was prepared from 502 mg (2 mmol) of monomer M6 and 216 mg (2 mmol) of 1,3-phenylenediamine M7 using the same polymerization method as for polyamide 13. Polymerization proceeded in clear solution. The resulting isolated polyamide 19a was soluble in polar solvents, such as NMP and DMAc. The inherent viscosity measured at 30°C concentration of 5 g/L in DMAc was 0.313 dL/g. Elemental analysis: Cal. C, 66.9%, H, 5.3%, N, 13.0% Obs. C, 65.0%, H, 5.6%, N, 12.3%. The IR spectrum and $_1$H NMR spectrum are shown in Fig. S7a and b, respectively.

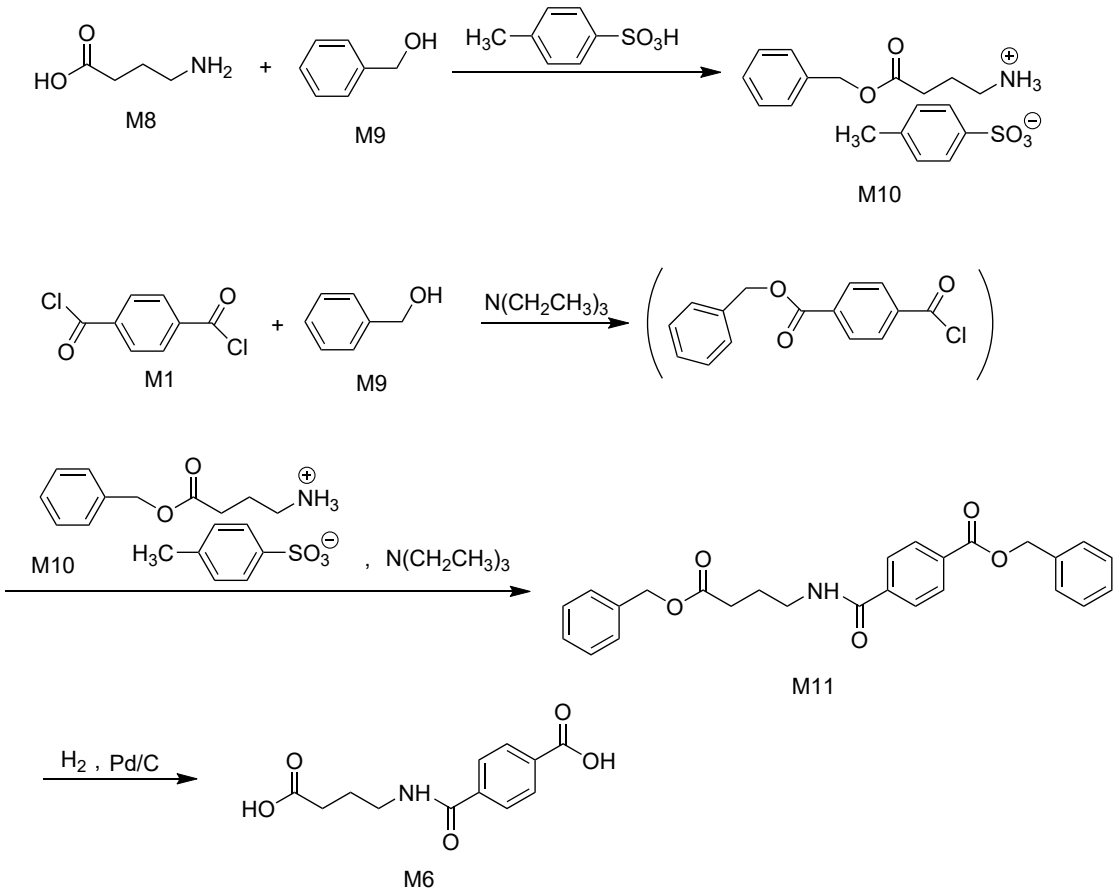

Figure S5: Synthetic route of monomer M6.

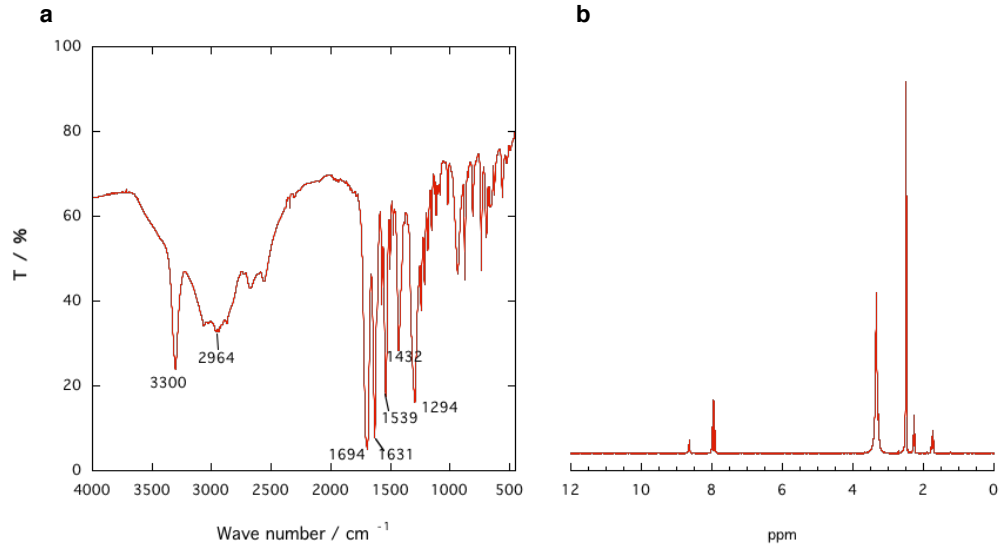

Figure S6: (a) FTIR spectrum for monomer M6. (b) ^{1}H NMR spectrum for monomer M6.

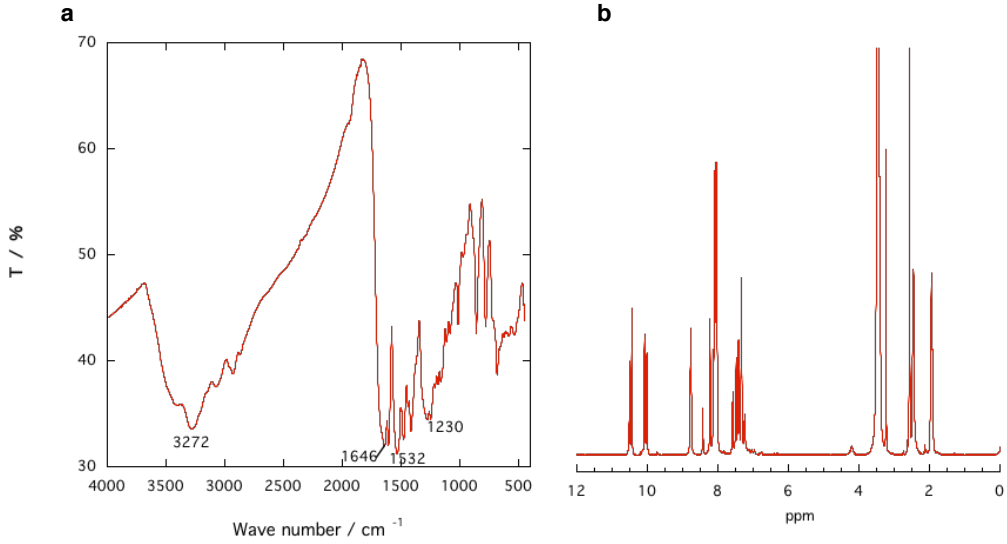

Figure S7: (a) FTIR spectrum for polymer 19a. (b) ^{1}H NMR spectrum for polymer 19a.

4.4 Characterization of polymers

Thermal analysis

The thermal properties of synthesized polymers 4, 13, and 19a were evaluated by DSC, TGA, TMA, and FSC. The specific heat capacities C_P of the polymers are shown in Fig. S8a. The glass transition temperature (T_g) of polymer 19a is approximately 194°C. Polymers 4 and 13 exhibited neither glass transition nor crystallization in the range of conditions of DSC. The TGA and TMA curves for polymers 4 and 13 are shown in Fig. S8b and c, respectively. The temperature at which 10% weight loss of polymer 13 occurred is higher than 500°C, indicating high thermal stability. Based on an ultra-fast temperature scan (30,000 K/s using FSC), the glass transition temperature T_g and melting temperature T_m are presented in Fig. S9. The predicted versus observed values of T_g and T_m for the synthetic polymers are displayed in Fig. S10.

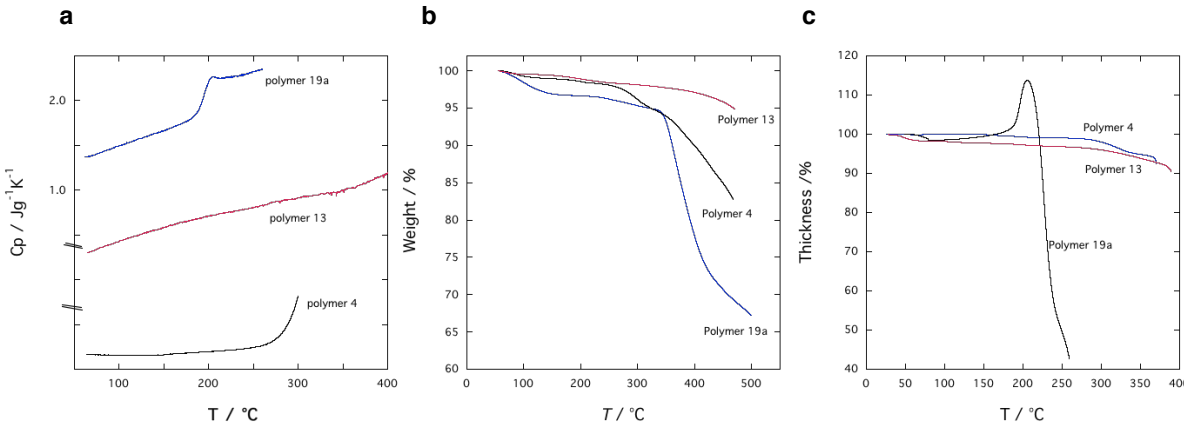

Figure S8: (a) DSC curves for polymers at a heating rate of 10°C/min under a nitrogen atmosphere, (b) TGA curves for polymers at a heating rate of 10°C/min under a nitrogen atmosphere, and (c) TMA curves for p

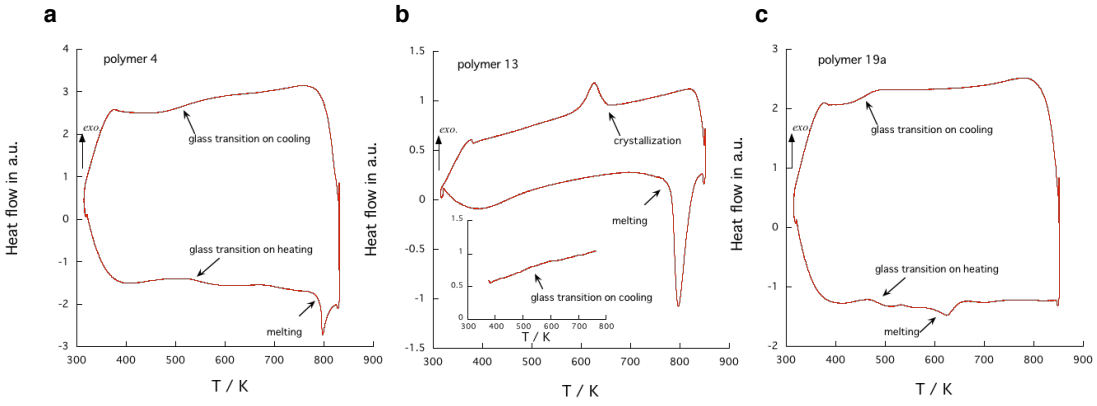

Figure S9: Fast scan DSC curves at a heating/cooling rate of 30,000 K/s under a nitrogen atmosphere for (a) polymer 4, (b) polymer 13, and (c) polymer 19a.

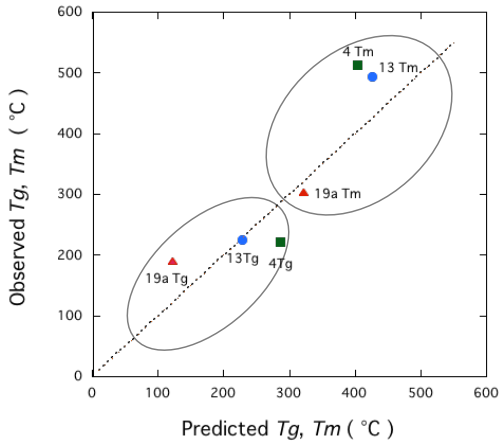

Figure S10: Correlation coefficients of predicted T_g and T_m compared to measured values determined by fast scanning calorimetry for the chemically synthesized polymers 4, 13, and 19a.

X-ray diffraction

In X-ray diffraction studies, polymer 19a was semi-amorphous, while polymers 4 and 13 were crystalline. X-ray diffraction patterns are shown in Fig. S11a–c, revealing crystallinities of 15.9%, 30.4%, and 9.3% for polymers 4, 13, and 19a, respectively. In addition, the crystallinity of polymer 4 was enhanced after annealing at 370°C for 10 min. The X-ray diffraction patterns of polymers 4 and 13 after annealing are shown in Fig. S11d and e. The crystallinity of polymer 4 increased to 45.1%, whereas no change was observed for polymer 13. This result is attributed to a crystal structural change (amide band disappearance) in polymer 4 resulting from a high-temperature chemical reaction observed in the FTIR spectrum in Fig. S12. The estimated reaction is shown [1] in Fig. S12c.

Temperature wave analysis

Thermal diffusivity was measured using temperature wave analysis. The phase difference between the input and output signals was measured as a function of the angular frequency of the input temperature wave, as shown in Fig. S13, for polymers 4, 13, and 19a. the changes before and after heat treatment of polymers 13 and 4 are shown together. In the experimental conditions of "thermal thick", the thermal diffusivity can be derived directly from the slope of the plot if the distance or sample thickness is known.

By introducing FSC [2], the T_g and T_m values of the aromatic polyamides were successfully observed for the first time, as shown in Fig. S9. Typically, these temperatures have not been observed because of the thermal degradation that occurred under conventional DSC. By using the scan rate of 30,000 K/s, Tm values higher than 400°C could be observed, and in parallel, cold crystallization phenomena could be observed in the case of polymer 13.

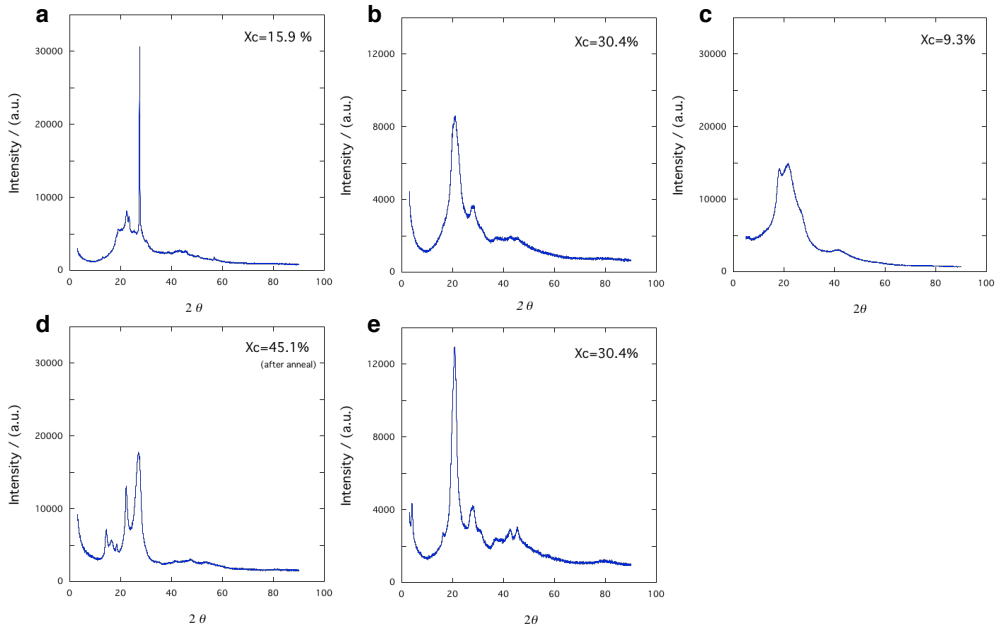

Figure S11: X-ray diffraction patterns of polymers using compressed pellets or powder: (a) polymer 4, (b) polymer 13, (c) polymer 19a. X-ray diffraction patterns of (d) polymer 4 after annealing at 400°C for 10 min, and (e) polymer 13 after annealing at 370°C for 10 min.

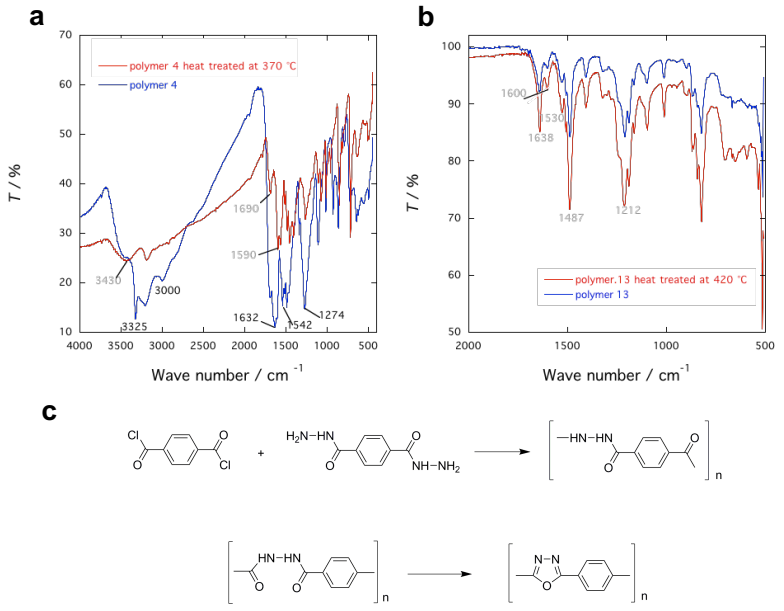

Figure S12: (a) Comparison of the FTIR spectrum of polymer 4 before and after annealing at 370°C. (b) Comparison of the ATR FTIR spectrum of polymer 13 before and after annealing at 420°C. (c) Estimated reaction of polymer 4 during annealing at 370°C.

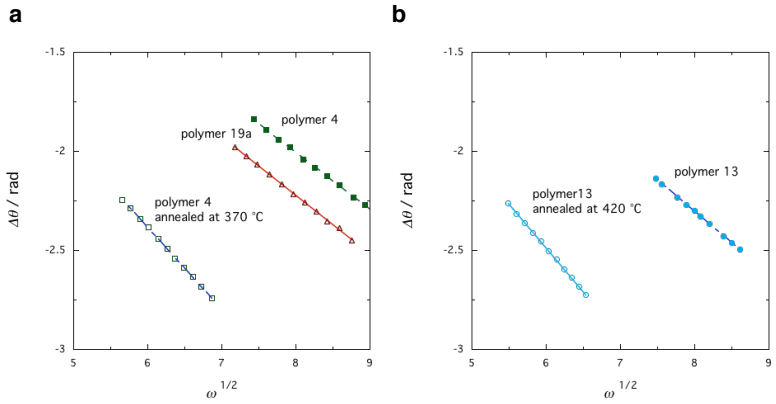

Figure S13: (a) Phase differences of (a) polymer 4 (thickness d = 165.2 μm, 301.2 μm (annealed at 370°C)), polymer 19a (d = 146.6 μm), and (b) polymer 13 (thickness d = 180.9 μm, 315.4 μm (annealed at 420°C)) plotted as a function of the square root of the angular frequency of the temperature wave.

References

[1] Bhausaheb V Tawade, Nitin G Valsange, and Prakash P Wadgaonkar. Synthesis and characterization of polyhydrazides and poly(1,3,4-oxadiazole)s containing multiple arylene ether linkages and pendent pentadecyl chains. *High Performance Polymers*, 29(7):836–848, 2017. doi: 10.1177/0954008316660368. URL `https://doi.org/10.1177/0954008316660368`.

[2] Y.L. Gao, E. Zhuravlev, C.D. Zou, B. Yang, Q.J. Zhai, and C. Schick. Calorimetric measurements of undercooling in single micron sized snagcu particles in a wide range of cooling rates. *Thermochimica Acta*, 482(1):1–7, 2009.